



X-Ray Shielding: Comparing Local Building Blocks For Optimal Radiation Protection In Jos, Nigeria

²Faith Igbe Adameh, ^{*1}Anil U.I. Sirisena, ²Eti-mnbuk Akanbi and ³Joseph Alih Adameh

¹Medical Physics Unit, Department of Radiology, Jos University Teaching Hospital, Jos, Nigeria.

²Department of Physics, University of Jos, Jos, Nigeria.

³Department of Building, University of Jos, Jos, Nigeria.

*Corresponding Author's E-Mail: shallom2k3@yahoo.com

ABSTRACT

Radiation protection from scattered X-rays is paramount in designing and constructing X-ray facilities. This study explored the half-value layers (HVLs) and linear attenuation coefficients of building blocks made from locally sourced soils: black soil (S₁), red soil (S₂), and brown soil (S₃) from Gwarandok, Giring Ward of Jos South local government area of Plateau State, Nigeria. The soils were analyzed for clay, sand, and silt content, and 10 cm x 10 cm blocks with varying thicknesses (1 cm to 4 cm) were produced. These blocks were subjected to X-rays (80 kVp, 10 mAs), and the transmitted radiation doses were measured using a Raysafe Thin-X Rad dose meter. A baseline free air exposure measurement was also taken with no block. Results revealed that blocks S₁, S₂, and S₃ had HVLs of 1.54 cm, 1.14 cm, and 1.36 cm, respectively, and linear attenuation coefficients of 0.45 cm⁻¹, 0.51 cm⁻¹, and 0.61 cm⁻¹, respectively. Notably, the red soil block (S₂) demonstrated the lowest HVL of 1.14 cm, outperforming the HVL of standard concrete (1.17 cm at 80 kVp). Conversely, the black soil block (S₁) exhibited the highest HVL of 1.54 cm. These findings indicate that red soil blocks from Gwarandok present an excellent alternative to concrete for X-ray shielding, providing an effective and cost-efficient solution. Moreover, the black and brown soil blocks also offer viable options, making all three types of locally made blocks practical choices for enhancing radiation protection in X-ray facility construction.

Keywords: Half value layer (HVL), linear and mass attenuation coefficients, X-ray shielding, building blocks, radiation protection.

INTRODUCTION

Ionizing radiation poses significant risks to human cells, making it essential to minimize exposure for both hospital staff and the public, particularly from the scattered radiation emanating from X-ray rooms (Benard, Sirisena, and Umar, 2024). Traditionally, materials like lead, concrete, and iron were commonly used to construct radiation barriers in hospital settings (Kalkornsurapranee et al., 2021). However, modern research is focused on developing environmentally friendly, cost-effective shielding materials that offer high density, superior attenuation coefficients, and low toxicity (Yilmaz et al., 2021). Additionally, hospitals that utilize ionizing radiation for diagnostic and therapeutic purposes must adhere to strict radiation protection standards when constructing X-ray facilities, ensuring compliance with legal and safety requirements set by relevant regulatory authorities (De Pires et al., 2024; Saidu et al., 2024). This study investigated the suitability of using locally made building blocks from different soil samples

which are environmentally friendly and cost effective since the soil is freely available as radiation barriers for scattered low-energy X-ray radiation to construct X-ray facilities.

The linear attenuation coefficient (μ) is a critical measure, indicating the fraction of incident photons in a monoenergetic beam that are attenuated per unit thickness of a material (Huda & Slone, 2003). This coefficient includes all interactions such as coherent scatter, Compton scatter, and the photoelectric effect, and is measured in cm^{-1} . The value of μ increases with the atomic number and physical density of the material but decreases with higher photon energy. Higher-density materials have higher linear attenuation coefficients, making them more effective for radiation shielding. The mass attenuation coefficient (μ/ρ) measures the probability of photon interaction per unit mass per unit area, expressed in $\text{cm}^2 \text{g}^{-1}$. Understanding the mass attenuation coefficients of X-rays and gamma rays in various materials is crucial for applications in industry, biology, agriculture, and medicine (Burcu & Salih, 2014).

When photons interact with matter, they can be transmitted unaffected, scattered in a different direction, or absorbed completely. The attenuation of X-rays is described by the equation (Bushburg et al., 2011):

$$I = I_0 e^{-\mu x}$$

Where, I is the intensity after attenuation, I_0 is incident intensity, μ is the linear attenuation coefficient (cm^{-1}), and x is the physical thickness of the absorber (cm).

The half-value layer (HVL) is the thickness of material needed to reduce the radiation intensity of an X-ray or gamma rays to half of its initial value and is given by (Bushburg et al., 2011):

$$HVL (cm) = \frac{0.693}{\mu}$$

MATERIALS AND METHODS

Three distinct soil types S_1 (black), S_2 (red), and S_3 (brown) were meticulously collected from various locations in Gwarandok, Giring Ward of Jos South Local Government Area, Plateau State, Nigeria. These samples underwent thorough analysis at a specialized soil testing laboratory to determine their clay, sand, and silt content.

To prepare the soil for block-making, each sample was carefully sieved to remove pebbles and stones. The soil was then mixed with water to achieve the right consistency for molding. The mixture was pressed into wooden frames, creating 10 cm x 10 cm blocks with thicknesses ranging from 1 cm to 4 cm. Each of the 12 blocks was labeled for easy identification and left to sun dry for a week, ensuring proper curing.

Once dried, the blocks were transported to an X-ray facility, equipped with a custom wooden stool to hold the blocks and a Raysafe Thin-X Rad dose meter for measurement. The blocks were placed one at a time between the X-ray source and the dose meter, aligned on the same axis. The setup is illustrated in Figures 1 and 2.

The X-ray source was set to 80 kVp and 10 mAs. An initial free air exposure dose (I_0) was recorded without any block in place. Subsequently, each block of varying thickness was positioned between the X-ray source and the dose meter. The dose meter measured the dose (I) of the X-ray beam after passing through the block, providing essential data for assessing the blocks' radiation attenuation properties.

All graphs were plotted using the IBM SPSS (Version 22) statistical software and the bar charts using the Microsoft Excel.

RESULTS

Table 1, presents the values of linear graph of $Y = \ln(I_0/I)$ against X (Thickness in cm) for block Samples S_1 (Black). Figure 3 shows this graph and from the graph as X increases the value of $\ln(I_0/I)$ increases. This indicates that the logarithmic value of intensities ratio has a linear relationship with the block thickness. The penetrated radiation of block sample S_{14} is out of range (not detectable by the dose meter) because radiation is minimally penetrating through it due to its larger thickness (4cm).

Table 2 and 3 show the values of $\ln(I_0/I)$ against X (Thickness in cm) for block Samples S_2 (Red) and S_3 (Brown). Figure 4 and 5 show these graphs respectively.

Table 4 presents the values for linear attenuation coefficients (μ) and half value layer (HVL) of the 3 block samples S_1 , S_2 , S_3 compared with that of concrete. The values for linear attenuation coefficient for each block samples S_1 , S_2 , S_3 ranged from 0.45 to 0.61 cm^{-1} and HVL ranged from 1.14 - 1.54 cm. Concrete at 80 kVp had linear attenuation coefficient of 0.59 cm^{-1} and HVL of 1.17 cm (CNDE, 2016).

Figure 6, presents the bar charts representing the linear attenuation coefficients and HVL of the 3 block samples compared with that of concrete at 80kVp.

Table 5, presents the values for mean densities, linear attenuation coefficients and mass attenuation coefficients of the block samples. The values for mass attenuation coefficient for each block samples S_1 , S_2 , S_3 ranged from 0.27 to 0.35 cm^2/g and C had 0.25 cm^2/g .

Table 6, shows the percentage of clay, silt and sand of the selected soil samples.

DISCUSSION

The linear attenuation coefficients (μ) for the 3 block samples produced in this study S_1 (produced from black soil), S_2 (produced from red soil), S_3 (produced from brown soil) were obtained to be 0.45, 0.51, and 0.61 cm^{-1} respectively while that of concrete was found to be 0.59 cm^{-1} . It was found that block S_1 had the lowest linear attenuation coefficients of the 3 block samples; this might be because it had the highest percentage of clay (16.83%) and lowest percentage of silt (0.28%). While block samples S_2 had the highest linear attenuation coefficient among the 3 block samples; this was probably so because it had the highest percentage of sand (87.84%) and a low percentage of clay (4.88%); also, S_2 possessed the highest density of the 3 blocks and this could make it stronger than the other 2 block samples. Moreover, the linear attenuation coefficient of the block sample S_2 was higher than that of the concrete having the linear attenuation coefficient of 0.59 cm^{-1} at 80 kVp (CNDE, 2016). The linear attenuation coefficient values obtained for the blocks from this study were slightly greater than that obtained by Jameel et al. (2010) [0.17 cm^{-1} and 0.15 cm^{-1} for white and red sand shields respectively]. A study carried out in FCT, Abuja showed the building blocks made from Abuja Municipal Area Council had the linear attenuation coefficient of 0.70 cm^{-1} (Benard, Sirisena and Umar, 2014).

Half value layer (HVL) ranged from 1.14 to 1.54 cm. The block sample with the highest HVL was S_1 with value of 1.54cm while HVL of concrete was found to be 1.17 cm (CNDE, 2016). HVL is an important parameter in designing any radiation shielding material since it indicates the required thickness of an absorber to reduce the radiation level to half of its initial value (Abdu et al., 2020).

Therefore, S_2 blocks can be used as the best substitute for solid concrete block and can be used as shielding material in construction of X-ray rooms.

CONCLUSION

The lower attenuation coefficient of block S_1 , attributed to its high clay and low silt content, contrasts with the superior performance of block S_2 , which boasts the highest attenuation coefficient due to its high sand content, low clay content, and greater density. Remarkably, block S_2 not only surpasses its soil-based counterparts but also outperforms concrete in terms of radiation shielding capabilities.

Therefore, S_2 blocks emerged as the most promising and effective alternative to traditional concrete blocks, particularly in the construction of X-ray rooms and other radiation-sensitive environments. However, from our findings all three types of locally made blocks used in this study can be practical choices for enhancing radiation protection in X-ray facility construction.

This study underscores the innovative potential of utilizing specific soil compositions in block production, offering a sustainable, viable, and potentially superior substitute to conventional concrete for radiation shielding in modern construction. The findings pave the way for more eco-friendly and cost-effective solutions in the realm of building materials, heralding a new era of sustainable construction practices.

REFERENCES

- Abdu, H. A., Pathan, J. M. & Ifra, F. (2020). Determination of Attenuation Coefficients of Some Selected Soil Samples by Using Gamma Energy at 0.360 MeV. *Journal of Chemistry*, 6(1): 2581-7507.
- Benard J.O., Sirisena U.A.I., and Umar I. (2024). Innovative Radiation Shielding: Performance Locally Made BaSO₄ – coated Building Blocks from FCT, Abuja as Low Cost Effective Barriers. *International Journal of Advanced Research*, 12(07): 852-858.
- Burcu A., & Salih Z. E. (2014) The Mass Attenuation Coefficients, Electronic, Atomic, and Molecular Cross Sections, Effective Atomic Numbers, and Electron Densities for Compounds of Some Biomedically Important Elements at 59.5 keV. *Science and Technology of Nuclear Installations*, 1-8.
- Bushburg J.T., Seibert J.A., Leidholdt Jr E.M. & Boone J.M. (2011). *The Essential Physics of Medical Imaging*. 3rd Ed., Lippincott Williams & Wilkins.
- CNDE (2016). Half-Value Layer, Center for Nondestructive Evaluation. www.nde-ed.org/X-Ray/HalfValueLayer.xhtml.
- De Pires M., Sobreira L.C., Maia I.Z., Rebeiro F.R., Rodriguez N.M., Souza E.G., Do Nascimento C.D. & Kulakowski M.P. (2024). Building Construction Materials For Ionizing Radiation Shielding: A Systematic Literature Review. *Cademo Pedagogico*, 21(1), 3129-3162.
- Huda, W., & Slone, R. M. (2003). *Review of Radiology Physics*. Lippincott Williams & Wilkins. 22-32.
- Jameel H., Omar D., Okla H., Ali B., & Turki A. (2010). Gamma Ray Shielding from Saudi White Sand. *Energy and Power Engineering*. 2(1): 6-9.
- Kalkornsurapranee E., Kothan S., Intom S., Johns J., Kaewjaeng S., Kedkaew C. et al., (2021). Wearable and Flexible Radiation Shielding Natural Rubber Composites: Effect of Different Radiation Shielding Fillers. *Radiation Physics and Chemistry*, 179, 109261.
- Saidu A., Abubakar A., Sokoto B. H., Umar M., Abubakar U., Usman F., & Bello G. (2024). Optimization of Shielding Barriers for Feasible Exposure to Medical X-ray radiation. *Caliphate Journal of Science and Technology*, 5(3), 280-287.
- Yilmaz, S.N., Abbey, I.K., Özdemir, T. (2021). A metal-ceramic-rubber composite for hybrid Gamma and neutron radiation shielding. *Radiation Physics and Chemistry*, 180, 109316.

FIGURES:



Figure 1: Well dried blocks of different soil samples.



Figure 2: Experimental set up showing the block sample and the radiation detector

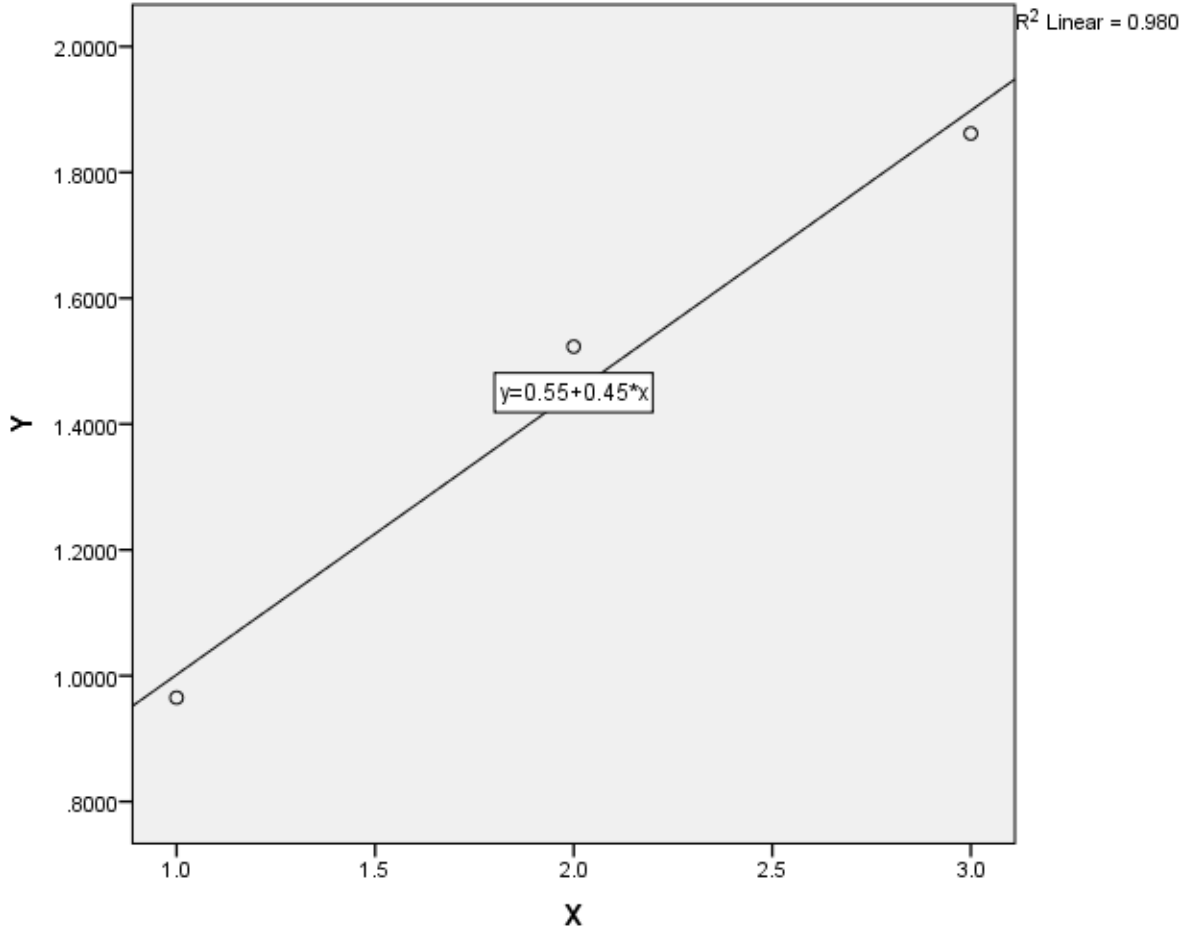


Figure 3: Linear graph between $Y = \ln(I_0/I)$ against X (Thickness in cm) for block Samples S₁

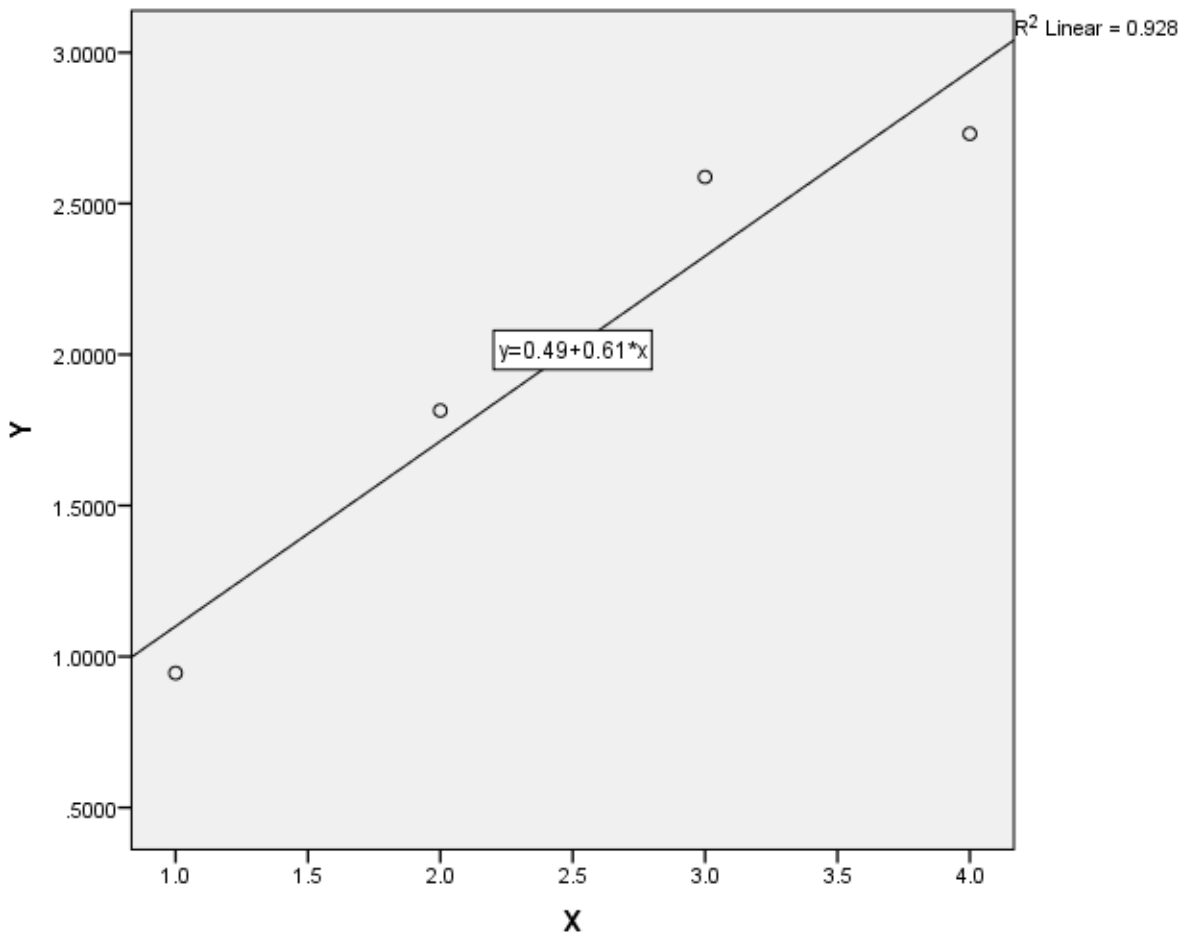


Figure 4: Linear graph between $Y = \ln(I_0/I)$ against X (Thickness in cm) for block samples S_2

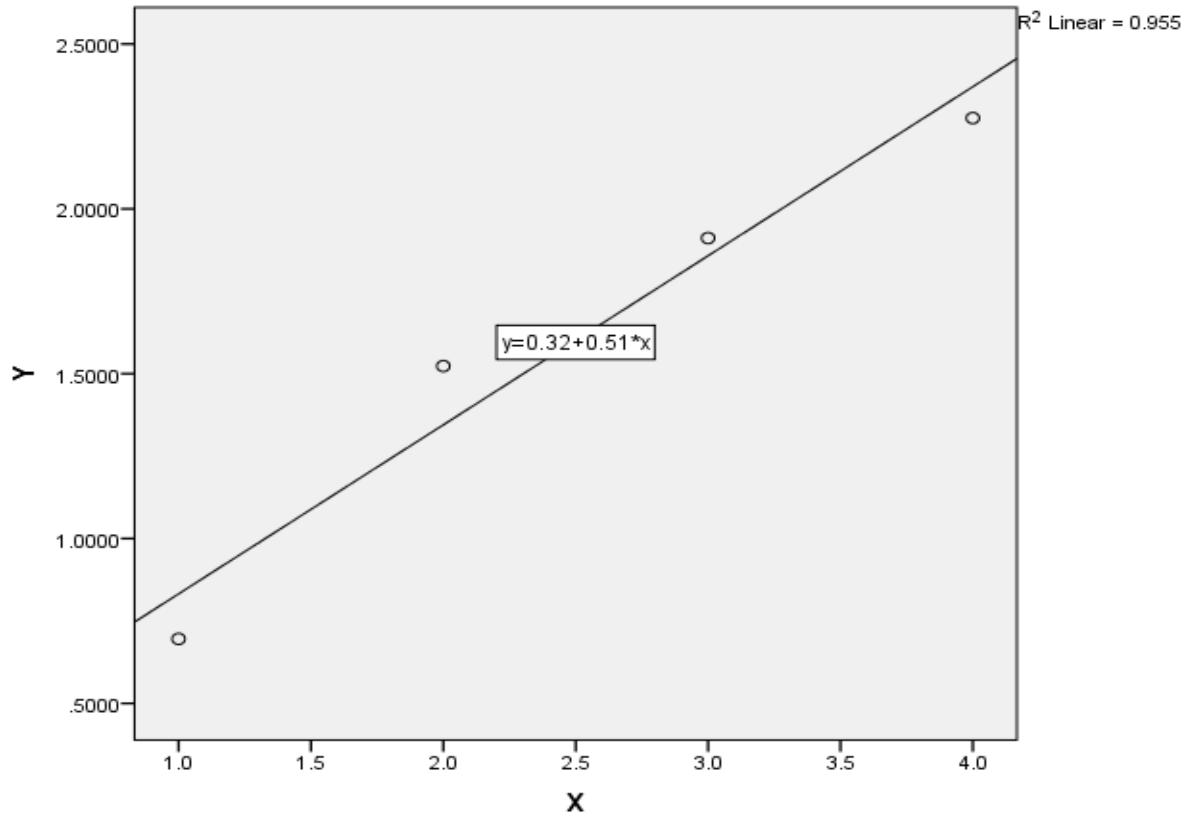


Figure 5: Linear graph between $Y = \ln(I_0/I)$ against X (Thickness in cm) for block samples S_3

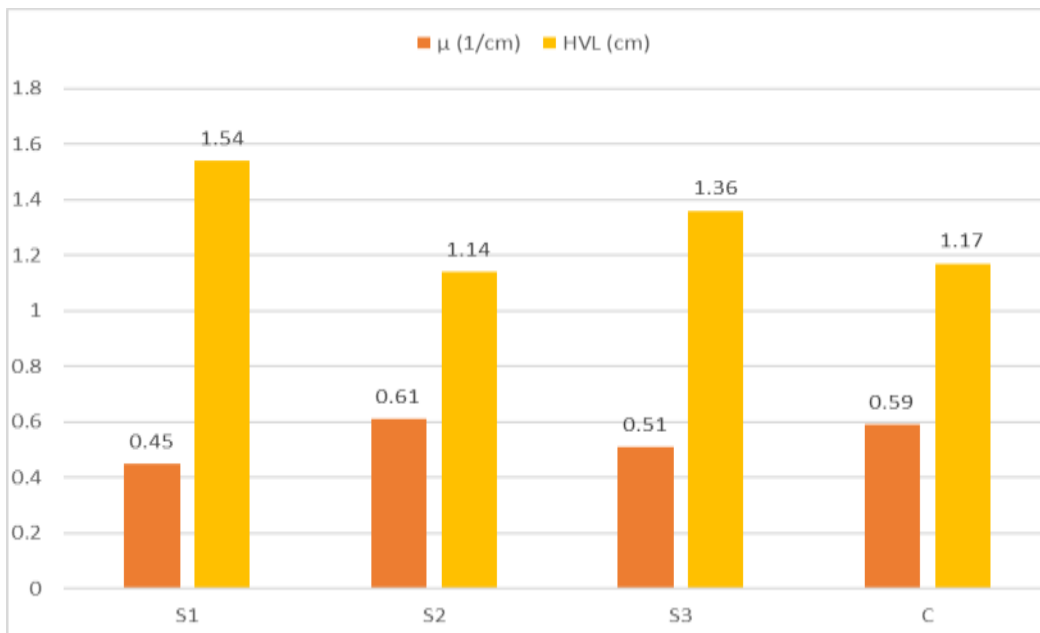


Figure 6: Bar Charts of Linear Attenuation Coefficients (μ) and HVL for the block samples

TABLES:

Table 1: Values for $\ln(I_0/I)$ against X (Thickness in cm) for block Samples S₁

Block sample	$I_0(\mu Gy)$	$I(\mu Gy)$	$\ln(I_0/I)$	$X(cm)$
S ₁₁	399.0	152.0	0.9651	1
S ₁₂	399.0	87.0	1.5231	2
S ₁₃	399.0	62.0	1.8618	3
S ₁₄	399.0	O/R	-	4

S₁₁=1cm, S₁₂=2cm, S₁₃=3cm, S₁₄=4cm

- O/R = out of range value (not detectable)

Table 2: Values for $\ln(I_0/I)$ against X (Thickness in cm) for block Samples S₂

Block sample	$I_0(\mu Gy)$	$I(\mu Gy)$	$\ln(I_0/I)$	$X(cm)$
S ₂₁	399.0	155.0	0.9455	1
S ₂₂	399.0	65.0	1.8146	2
S ₂₃	399.0	30.0	2.5878	3
S ₂₄	399.0	26.0	2.7309	4

S₂₁=1cm, S₂₂=2cm, S₂₃=3cm, S₂₄=4cm

Table 3: Values for $\ln(I_0/I)$ against X (Thickness in cm) for block Samples S₃

Block sample	$I_0(\mu Gy)$	$I(\mu Gy)$	$\ln(I_0/I)$	$X(cm)$
S ₃₁	399.0	199.0	0.6956	1
S ₃₂	399.0	87.0	1.5231	2
S ₃₃	399.0	59.0	1.9114	3
S ₃₄	399.0	41.0	2.2754	4

S₃₁=1cm, S₃₂=2cm, S₃₃=3cm, S₃₄=4cm

Table 4: Values for linear attenuation coefficients (μ) and half value layer (HVL) of block samples compared with Concrete at 80 kVp

Block sample	$\mu (cm^{-1})$	HVL (cm)
S ₁	0.45	1.54
S ₂	0.61	1.14
S ₃	0.51	1.36
C	0.59	1.17

Table 5: Mean densities, linear attenuation coefficients and mass attenuation coefficients

Sample	$\mu(\text{cm}^{-1})$	Mean density $\rho (\text{g}/\text{cm}^3)$	Mass atten. μ/ρ
S ₁	0.45	1.64	0.27
S ₂	0.61	1.72	0.35
S ₃	0.51	1.65	0.31
C	0.59	2.40	0.25

Table 6: Percentage of clay, silt and sand of the three soil samples used in study

Sample	Clay	Silt	Sand	Textural class
S ₁	16.83	0.28	82.84	Sandy loam
S ₂	4.88	7.28	87.84	Loamy sand
S ₃	4.88	8.28	86.84	Loamy sand